Current Science
CS 5 (4), 3948-3959 (2025)
Received 11 May 2025 | **Revised 12 June** 2025 | **Accepted 15 July**. 2025 | **Online Available 13 August** 2025
https://doi.org/ 10.52845/CS/2025-5-4-50

Current Science

Current Science

OPEN ACCESS

ISSN(O) 2795-8639

Original Article

IGFBP3 as a Potential Biomarker and Therapeutic Target in Hepatocellular Carcinoma: A Multi-Cohort Analysis

Yunji Xu[1], Xupeng Chen[2], Shenpeng Li[3], Wenbing Li[1], Yin Tao[2,4,*]

[1]Department of General Surgery, The Second Affiliated Hospital, Hengyang Medical College, University of South China, Hengyang, Hunan,421001, China

[2]Department of Clinical Laboratory, Zhuzhou Central Hospital, Zhuzhou, Hunan, 421000, China

[3]Department of rehabilitation medicine, Zhuzhou Central Hospital, Zhuzhou, Hunan, 421000, China

[4]Department of General surgery, Zhuzhou Central Hospital, Zhuzhou, Hunan, 421000, China

[*]Corresponding Author: Yin Tao

Abstract:

Objective: This study aimed to investigate the expression patterns and prognostic significance of insulin-like growth factor-binding protein 3 (IGFBP3) in hepatocellular carcinoma (HCC) and other cancer types.

Methods: IGFBP3 expression profiles and clinical data from The Cancer Genome Atlas (TCGA)-LIHC, International Cancer Genome Consortium (ICGC-LIRI-JP), Gene Expression Omnibus (GEO; GSE102079/GSE112790), and Genotype-Tissue Expression (GTEx) databases were integrated. Experimental validation was performed using immunohistochemistry (IHC) and qRT-PCR to compare IGFBP3 expression between HCC and adjacent non-tumor tissues. Survival analysis was conducted using Kaplan-Meier curves for both TCGA and ICGC cohorts. Immune infiltration correlations were assessed using ESTIMATE and TIMER algorithms. Pan-cancer analysis was conducted using TCGA data.

Results: IGFBP3 expression was significantly downregulated in HCC across multiple cohorts (TCGA, ICGC, and GEO) and experimental validation (IHC and qRT-PCR) ($p<0.01$). Its expression positively correlated with advanced clinical stage: elevated IGFBP3 levels were observed in late-stage (III–IV) and higher T-stage tumors (TCGA-LIHC, $p < 0.01$), and high expression was more frequent in poorly differentiated (G3–G4) tumors. Importantly, overexpression of IGFBP3 correlated significantly with poorer overall survival (TCGA: p=0.004, HR=1.666 [95% CI 1.176–2.360]; ICGC: p=0.0009, HR=4.631 [95% CI 1.688–12.71]) and progression-free survival (TCGA: p=0.014, HR=1.734 [95% CI 1.118–2.688]). Mechanistically, IGFBP3 expression was positively correlated with B cell and macrophage infiltration (r=0.39, $p<0.0001$). Pan-cancer analysis revealed tissue-specific dysregulation of IGFBP3 with varying expression levels and prognostic implications for different tumor types.

Conclusion: IGFBP3 was low expression in HCC. However, elevated IGFBP3 correlates with advanced disease, specific subgroups (female, age<40), and serves as a robust independent predictor of poor prognosis. IGFBP3 also associates with immune infiltration (B cells, macrophages) and exhibits tissue-specific dysregulation across cancers, establishing it as a valuable prognostic biomarker and potential therapeutic target in HCC.

Keywords: Hepatocellular carcinoma, IGFBP3, Biomarker, Prognosis, Immune infiltration

1. Introduction

Hepatocellular carcinoma (HCC) is a significant global health concern owing to its aggressive nature and poor prognosis. It is the fourth leading cause of cancer-related mortality worldwide, with

approximately 905,700 new cases and 830,200 deaths reported annually [1]. In China, HCC accounts for nearly 45% of global cases and 50% of deaths, reflecting a disproportionately high burden associated with endemic hepatitis B virus (HBV) infections and environmental carcinogens, such as aflatoxin B1 [2]. The incidence of HCC varies significantly between regions. High-risk areas include East Asia, sub-Saharan Africa, and Southeast Asia, where HBV and aflatoxin exposure is prevalent [1]. Conversely, Western countries are experiencing increasing HCC rates due to hepatitis C virus (HCV) infection, non-alcoholic fatty liver disease (NAFLD), and alcohol abuse [3]. China's HCC mortality rate remains alarmingly high, with age-standardized incidence rates of 18.3 per 100,000 in males and 6.6 per 100,000 in females, HBV vaccination coverage and delayed diagnosis [2].

Key risk factors for HCC include chronic HBV/HCV infection, metabolic disorders (e.g., NAFLD and diabetes), excessive alcohol consumption, and exposure to environmental toxins [3,4]. Despite advancements in surveillance techniques (e.g., ultrasound and alpha-fetoprotein [AFP] testing), over 70% of patients with LIHC are diagnosed at advanced stages, rendering curative therapies (such as resection and transplantation) ineffective [5]. First-line systemic therapies, including tyrosine kinase inhibitors (sorafenib and lenvatinib) and immune checkpoint inhibitors (atezolizumab + bevacizumab), extend the median survival to 12–19 months. However, these treatments do not address long-term recurrence (up to 70% within 5 years) or drug resistance [6,7]. The 5-year survival rate for LIHC remains below 20%, decreasing to <5% in metastatic cases [5]. Tumor heterogeneity, dysregulated signaling pathways (e.g., insulin-like growth factor [IGF] and Wnt/β-catenin), and immunosuppressive microenvironments further complicate treatment efficacy [8,9].

The limitations of current therapies highlight the urgent need for molecular targeted strategies to improve treatment outcomes. Insulin-like growth factor-binding protein 3 (IGFBP3), a multifunctional regulator of cell proliferation, apoptosis, and metastasis, has emerged as a promising candidate for this purpose [10]. IGFBP3 exhibits context-dependent roles in cancer, acting as both a tumor suppressor (via Wnt/β-catenin inhibition) and a promoter (through IGF-1R-independent signaling). Its interactions with HCC-associated pathways make it a critical therapeutic target [11]. Recent studies have indicated that IGFBP3 overexpression suppresses HCC progression by antagonizing oncogenic Wnt signaling, whereas its downregulation is correlated with chemoresistance and poor prognosis [12]. Elucidating IGFBP3's dual roles in HCC could unlock strategies for overcoming drug resistance, mitigating recurrence, and improving survival outcomes.

In this study, we analyzed IGFBP3 expression, clinical characteristics, and prognosis using TCGA-LIHC and ICGC-LIRI-JP datasets. These findings were experimentally validated using immunohistochemistry (IHC) and quantitative reverse transcription polymerase chain reaction (qRT-PCR) in HCC specimens. Additionally, we investigated the correlation between IGFBP3 expression and immune cell infiltration as well as the enriched pathways. Finally, the expression and prognostic significance of IGFBP3 were analyzed in pan-cancer to provide a comprehensive understanding of its role in HCC and potential therapeutic implications.

2. Materials and methods

2.1 Data collection

IGFBP3 transcriptome data and clinical information for HCC were retrieved from four independent cohorts: (1) The Cancer Genome Atlas (TCGA-LIHC; https://portal.gdc.cancer.gov), (2) International Cancer Genome Consortium-LIRI-JP (ICGC-LIRI-JP ; https://dcc.icgc.org), and (3) Gene Expression Omnibus (GEO) datasets: a. GSE102079 and b. GSE11 2790 (https://www.ncbi.nlm.nih.gov/geo/). Additionally, pan-cancer IGFBP3 expression profiles (36 cancer types) and overall survival (OS) data were extracted from TCGA (https://www.cancer.gov/ccg/research/genome-sequencing/tcga). The workflow of this study is illustrated in Figure 1.

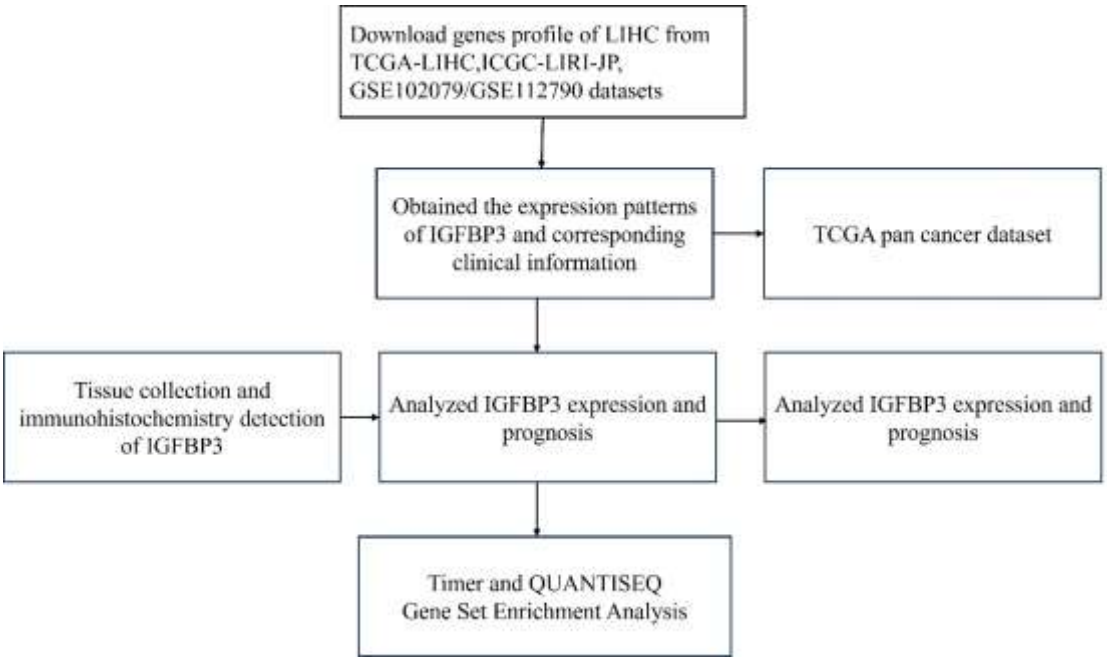

Figure 1: Schematic representation of the study workflow.

Analysis of IGFBP3 expression patterns and survival parameters

RNA-seq raw count data and clinical annotations for HCC were downloaded from TCGA, ICGC, and GEO platforms using TCGAbiolinks (v3.14.1) and GEOquery (v2.66.0). Samples with missing IGFBP3 expression values or incomplete survival records (OS < 30 d) were excluded. IGFBP3 expression levels were normalized using transcripts per million (TPM) and stratified into high and low groups using the median as a cutoff value. Prognostic significance was assessed using Kaplan-Meier survival analysis with log-rank tests in TCGA and ICGC cohorts.

2.3 Immune Cell Infiltration Analysis

TIMER

The abundance of immune cell subsets in TCGA-LIHC tumor samples was quantified using TIMER 2.0, a web platform (http://timer.cistrome.org/) [13]. Bulk RNA-seq data (FPKM normalized and log2-transformed) from TCGA-LIHC were analyzed using TIMER's constrained least-squares regression model to deconvolute six immune cell types: B cells, CD4+ T cells, CD8+ T cells, neutrophils, macrophages, and dendritic cells. Tumor purity was automatically adjusted using TIMER's pre-computed models to minimize confounding effects. The correlation between IGFBP3 expression (log2-transformed TPM values) and immune cell infiltration levels was evaluated using Spearman's rank correlation, with significance set at *p* < 0.05.

QUANTISEQ

The quanTIseq computational framework [14] was used to estimate the absolute immune cell densities (cells/mm²) in TCGA-LIHC samples. Raw RNA-seq reads (FASTQ files) were aligned to the GRCh38 reference genome using STAR v2.7.10a, and gene-level counts were generated using featureCounts v2.0.3. Expression matrices were normalized using the trimmed mean of M-values (TMM) method to correct for compositional biases. The quanTIseq deconvolution model, which uses linear least-squares regression with immune cell-specific signature matrices (including M1/M2 macrophages and regulatory T cells), was executed using quanTIseq R package. To validate the immune cell estimates, IHC results from matched LIHC tissue sections were compared with computational predictions.

2.4 Tissue Collection

Eight paired HCC and adjacent non-tumor tissues (≤2 cm from the tumor margin) were obtained from treatment-naïve patients who underwent curative resection at Zhuzhou Central Hospital (Hunan, China) between 2020-2022. All specimens were pathologically confirmed by two independent histopathologists at the hospital. The study protocol (No. LLYPJ2025044-01) was approved by the Institutional Review Board, and written informed consent was obtained from all

participants, in accordance with the Declaration of Helsinki.

2.5 qRT-PCR and IHC

qRT-PCR: Total RNA was extracted using TRIzol (Invitrogen, #15596026), reverse-transcribed using PrimeScript RT Master Mix (Takara, #RR036A), and amplified using QuantStudio 5 (Thermo Fisher), with β-actin serving as the endogenous control. Primer sequences are listed in Table 1. Relative expression of IGFBP3 was calculated using the 2−ΔΔCT method.

Table 1, RT-PCR primer information

Gene name	Primer sequence (5'- 3')
H-GAPDH-S	GGAAGCTTGTCATCAATGGAAATC
H-GAPDH-A	TGATGACCCTTTTGGCTCCC
H-IGFBP3-F	AGACACACTGAATCACCTGAAGT
H-IGFBP3-R	AGGGCGACACTGCTTTTTCTT

IHC: Formalin-fixed paraffin-embedded sections were subjected to antigen retrieval (citrate buffer, pH 6.0) and blocked with 10% goat serum. The slides were incubated overnight with anti-IGFBP3 antibody (Abcam, #ab313875; 1:200), followed by incubation with horseradish peroxidase (HRP)-conjugated secondary antibody and DAB visualization. ImageJ (v1.53) was used to calculate the integrated optical density (IOD) normalized to the tissue area.

2.6 Statistical Analysis

Continuous variables were compared using the Student's t-test for normally distributed data or the Mann-Whitney U test for non-normally distributed data. Survival differences were analyzed using the log-rank test with Kaplan-Meier curves. Multivariate Cox regression results are presented as hazard ratios (HR) with 95% confidence intervals (CI). All analyses were performed using R (v4.3.1), with statistical significance defined as two-tailed $p < 0.05$ or false discovery rate (FDR) < 0.05 for multiple comparisons.

3. Results

3.1 Downregulation of IGFBP3 in HCC

The expression of IGFBP3 was significantly reduced in HCC compared to that in normal liver tissue, as evidenced by multiple datasets: TCGA-LIHC, ICGC-LIRI-JP, GSE102079, and GSE112790 (all $p < 0.0001$, Figures 2A-D). This finding was further corroborated by qRT-PCR and IHC analyses conducted on eight pairs of fresh HCC and adjacent normal tissues, which confirmed a marked downregulation of IGFBP3 in HCC (all $p < 0.01$, Figure 2 E-G).

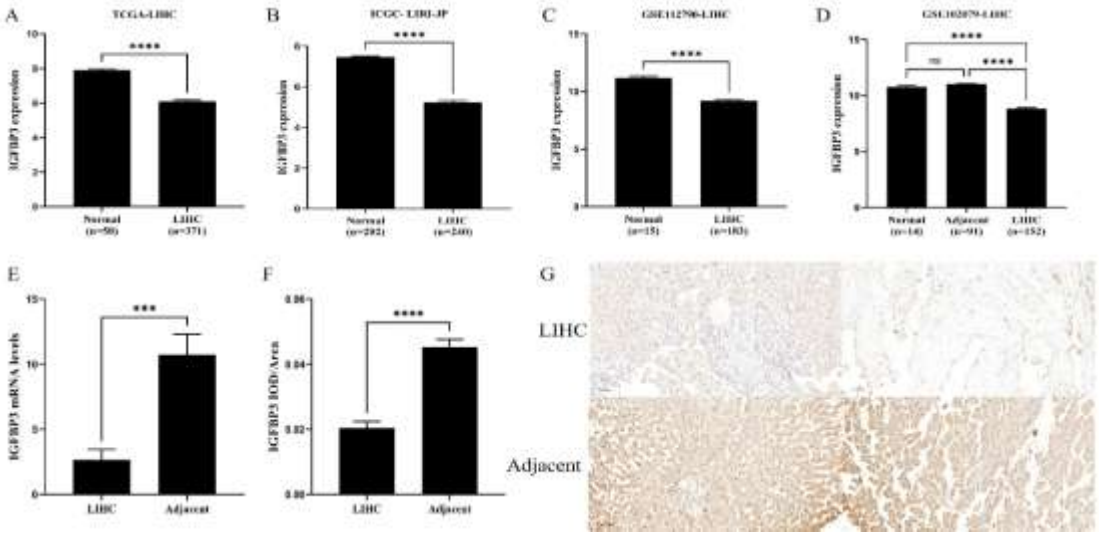

Figure 2: Expression analysis of IGFBP3 in HCC. (A-D): Comparative analysis of IGFBP3 expression in HCC and normal liver tissues. (E-G): Validation of IGFBP3 downregulation in HCC tissues using qRT-PCR and IHC.

3.2 Correlation of IGFBP3 expression with clinical classification of HCC

The correlation between IGFBP3 expression and various clinical parameters were by analyzed. In the TCGA-LIHC dataset, IGFBP3 expression was significantly elevated in advanced tumor stages (III-IV) compared to earlier stages (Stage I vs. II: $p<0.01$; Stage I vs. III-IV: $p<0.001$) and in higher T stages (T1 vs. T2: $p<0.01$; T1 vs. T3-T4: $p<0.001$). Elevated IGFBP3 expression was also observed in high-grade tumors (G3-G4) versus lower grades (G1 vs. G3-G4: $p<0.05$; G2 vs. G3-G4: $p<0.05$). Furthermore, IGFBP3 expression was significantly lower in male patients and in patients aged >40 years ($p<0.05$ and $p<0.01$, respectively). These findings were partially validated in the ICGC-LIRI-JP cohort, where elevated IGFBP3 expression was confirmed in stage IV HCC relative to stage I and stage II tumors (Stage I vs. IV: $p<0.05$; Stage II vs. IV: $p<0.05$; Figure 3F).

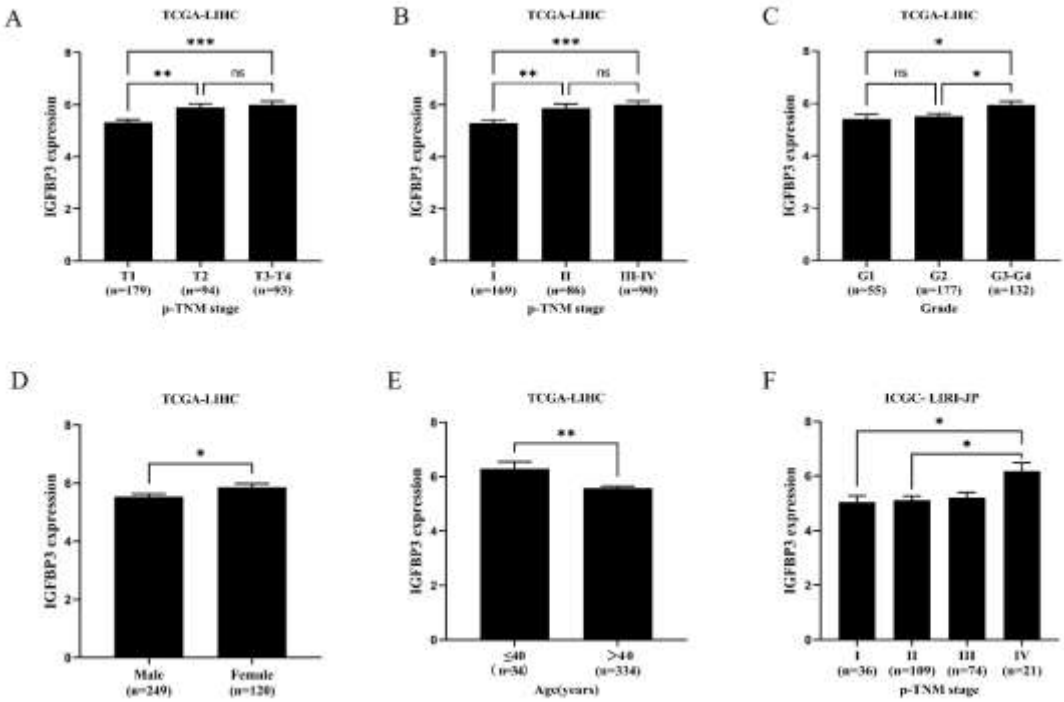

Figure 3: Association of IGFBP3 expression with clinical classification in HCC. (A-E): IGFBP3 expression shows significant associations with age, gender, histological grade, and tumor stage in the TCGA-LIHC cohort, respectively. (F): In the ICGC-LIRI-JP cohort, IGFBP3 expression significantly correlates with tumor stage.

3.3 Effect of IGFBP3 Expression on Prognosis in HCC

In both the TCGA-LIHC and ICGC-LIRI-JP cohorts, patients with HCC exhibiting high IGFBP3 expression demonstrated significantly shorter overall survival (OS) and progression-free survival (PFS) compared to those with low expression levels. In TCGA-LIHC, high IGFBP3 was associated with worse OS ($p = 0.004$; HR = 1.666, 95% CI: 1.176–2.360) and PFS ($p = 0.014$; HR = 1.734, 95% CI: 1.118–2.688). Similarly, in the ICGC-LIRI-JP cohort, high IGFBP3 was associated with worse OS ($p = 0.0009$; HR = 4.631, 95% CI: 1.688–12.710) (Figures 4A–C).

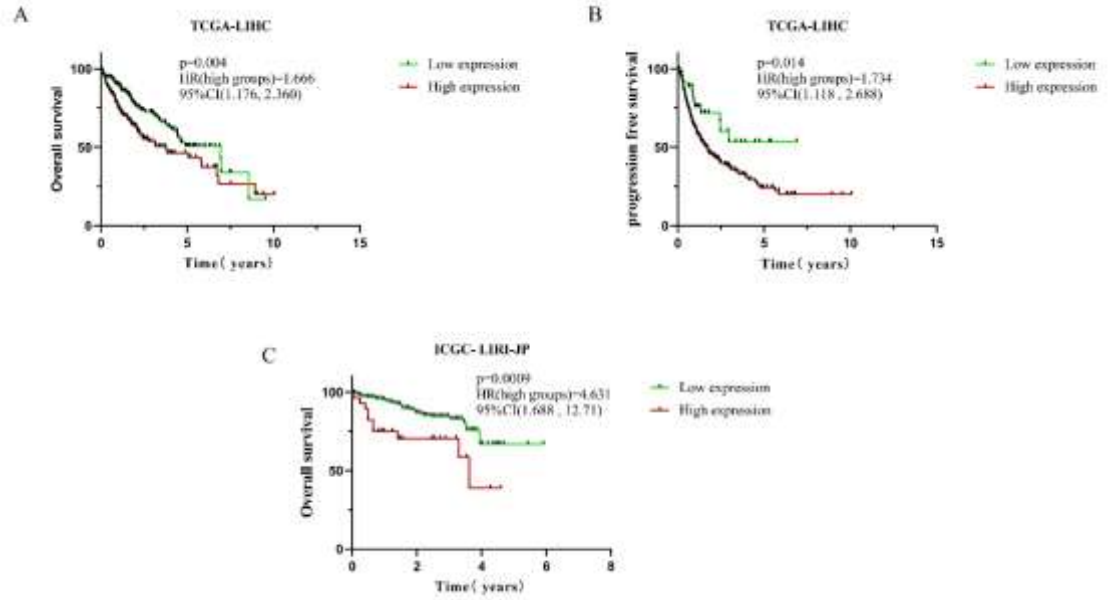

Figure 4: Prognostic value of IGFBP3 expression in HCC. (A, B): Kaplan-Meier curves comparing overall survival (OS) and progression-free survival (PFS) between HCC patients with high vs. low IGFBP3 expression in the TCGA-LIHC cohort. (C): Kaplan-Meier curve comparing overall survival (OS) between HCC patients with high vs. low IGFBP3 expression in the ICGC-LIRI-JP cohort.

3.4 Correlation of IGFBP3 Expression with Immune Cell Infiltration and Enriched Pathways in HCC

An analysis of immune cell infiltration using the TIMER and QUANTISEQ algorithms on the TCGA-LIHC dataset revealed significant correlations between IGFBP3 expression and various immune cell populations (Figure 5A-B). The TIMER algorithm demonstrated strong positive correlations with (Figure 5 A) ($p < 0.0001$) neutrophils ($r = 0.49$), macrophages ($r = 0.39$), CD4+ T cells ($r = 0.36$), dendritic cells (DCs, $r = 0.33$), and B cells ($r = 0.27$). A moderate positive correlation ($p < 0.05$) was observed with CD8+ T cells ($r = 0.10$). QUANTISEQ algorithm analysis further dissected macrophage subsets and identified positive correlations (Figure 5 B) with M1 macrophages ($r = 0.37$, $p < 0.0001$), M2 macrophages ($r = 0.26$, $p < 0.0001$), B cells ($r = 0.23$, $p < 0.0001$), and regulatory T cells (Tregs, $r = 0.26$, $p < 0.0001$), as well as moderate positive correlations with CD4+ T cells ($r = 0.11$, $p < 0.05$), CD8+ T cells ($r = 0.13$, $p < 0.05$), and dendritic cells ($r = 0.13$, $p < 0.05$). A negative correlation was observed with "Other cells" ($r = -0.32$, $p < 0.0001$). Gene Set Enrichment Analysis (GSEA) of the TCGA-LIHC dataset identified several significantly enriched pathways associated with IGFBP3 expression (Figure 5 C), including PRION_DISEASES (ES=0.6980, NP=0.0000), JAK_STAT_SIGNALING_PATHWAY (ES=0.6000, NP=0.0000), TOLL_ LIKE_RECEPTOR_ SIGNALING_PATHWAY (ES=0.5580, NP=0.0000), NATURAL_KILLER_CELL_MEDIATED_CYTOTOXICITY (ES=0.5496, NP=0.0060), RENAL_CELL_CARCINOMA (ES=0.5713, NP=0.0021), TGF_BETA_SIGNALING_PATHWAY (ES=0.5439, NP=0.0021), APOPTOSIS (ES=0.4857, NP=0.0020), VASCU LAR_ SMOOTH_MUSCLE_CONTRACTION (ES=0.4887, NP=0.0165), MAPK_SIGNALING_ PATHWAY (ES=0.4385, NP=0.0040), and B_CELL_RECEPTOR_SIGNALING_PATHWAY (ES=0.5480, NP=0.0042).

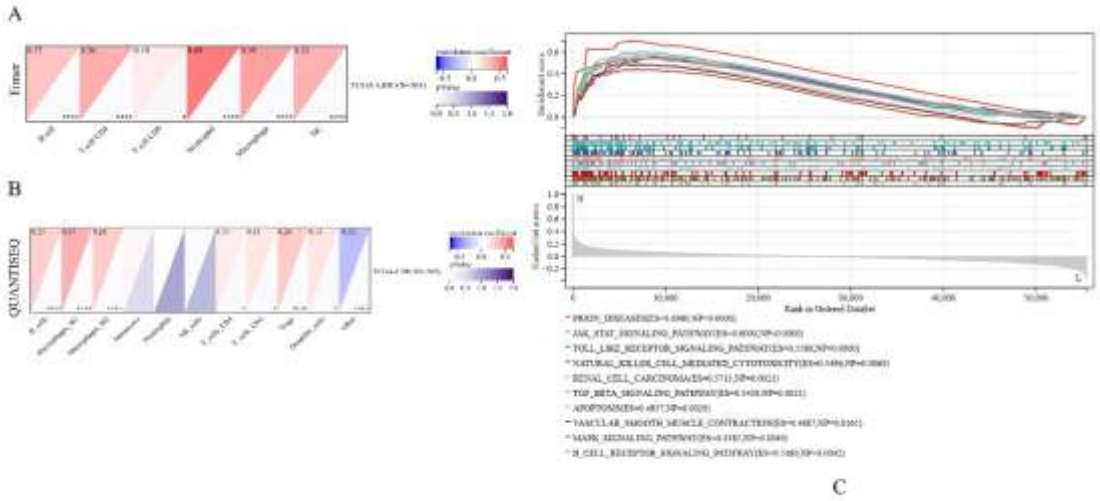

Figure 5: Association of IGFBP3 expression with immune infiltration and pathway enrichment in HCC. (A, B): Correlation between IGFBP3 expression and immune cell infiltration levels in the TCGA-LIHC cohort analyzed using TIMER and QUANTISEQ algorithms. (C): Gene Set Enrichment Analysis (GSEA) of hallmark pathways associated with IGFBP3 expression in TCGA-LIHC.

Pan-Cancer Analysis of IGFBP3 Expression and Prognostic Significance

Analysis of IGFBP3 expression across multiple cancer types in TCGA pan-cancer cohort revealed differential expression patterns. Downregulation was observed in uterine corpus endometrial carcinoma (UCEC), breast invasive carcinoma (BRCA), prostate adenocarcinoma (PRAD), LIHC, skin cutaneous melanoma (SKCM), ovarian serous cystadenocarcinoma (OV), uterine carcinosarcoma (UCS), kidney chromophobe (KICH), and cholangiocarcinoma (CHOL) (Figure 6A and Table 2).

Table 2, The expression of IGFBP3 in Pan-Cancer

Cohort	Expression		p
	Tumor	Normal	
TCGA-GBM	6.78±1.71	2.05±1.84	2.0e-80
TCGA-GBMLGG	4.89±2.11	2.05±1.84	1.4e-137
TCGA-LGG	4.33±1.88	2.05±1.84	1.5e-93
TCGA-LUAD	6.93±1.43	5.03±1.32	1.3e-74
TCGA-ESCA	6.37±1.49	4.81±1.58	2.0e-32
TCGA-STES	6.50±1.32	4.72±1.64	7.7e-109
TCGA-KIPAN	8.48±2.42	6.27±1.78	1.3e-27
TCGA-COAD	5.80±1.21	5.46±2.03	0.01
TCGA-COADREAD	5.84±1.18	5.45±2.00	1.1e-3
TCGA-STAD	6.57±1.24	4.41±1.77	1.6e-57
TCGA-HNSC	6.70±1.53	5.00±1.61	5.3e-10
TCGA-KIRC	9.90±1.46	6.27±1.78	5.7e-70
TCGA-LUSC	7.53±1.62	5.03±1.32	8.0e-92
TCGA-BLCA	8.15±1.95	7.01±1.20	4.2e-4
TCGA-PAAD	7.83±1.43	2.15±1.86	8.9e-55
TCGA-TGCT	5.20±1.82	3.58±1.22	7.2e-16)
TCGA-LAML	-0.34±2.29	-0.99±1.80	2.1e-6
TCGA-PCPG	5.64±1.71	2.01±1.33	5.2e-3
TCGA-ACC	5.86±1.35	2.18±1.60	1.6e-29

TCGA-UCEC	7.30±1.28	8.25±1.65	4.2e-3
TCGA-BRCA	6.04±1.00	7.43±0.94	3.0e-75
TCGA-PRAD	5.34±1.06	6.13±0.93	3.3e-15
TCGA-LIHC	5.65±1.47	7.23±0.94	2.1e-31
TCGA-SKCM	5.45±1.72	6.56±1.28	8.6e-13
TCGA-OV	6.15±1.42	7.36±1.35	5.6e-14
TCGA-UCS	7.51±0.97	8.05±1.15	9.5e-3
TCGA-ALL	4.68±3.64	0.99±1.80	1.2e-26
TCGA-KICH	5.42±1.71	6.27±1.78	3.3e-4
TCGA-CHOL	5.74±1.47	7.45±0.40	6.6e-4

No significant differences in expression were noted in cervical squamous cell carcinoma (CESC), kidney renal papillary cell carcinoma (KIRP), thyroid carcinoma (THCA), or rectal adenocarcinoma (READ).

Prognostic analysis further revealed that (Figure 6B and Table 3) high IGFBP3 expression was associated with poor prognosis in glioblastoma and low-grade glioma (GBMLGG), lower-grade glioma (LGG), pan-kidney cohort (KIPAN), kidney renal papillary cell carcinoma (KIRP), LIHC, pancreatic adenocarcinoma (PAAD), lung adenocarcinoma (LUAD), and colorectal adenocarcinoma (COADREAD). Notably, in HCC, IGFBP3 exhibited a distinct pattern: while its expression was significantly downregulated (Figure 6A), it concurrently functioned as a high-risk prognostic factor (Hazard Ratio [HR] = 1.21; Figure 6B, Table 3). This suggests IGFBP3 plays a complex, context-dependent dual role in liver cancer progression.

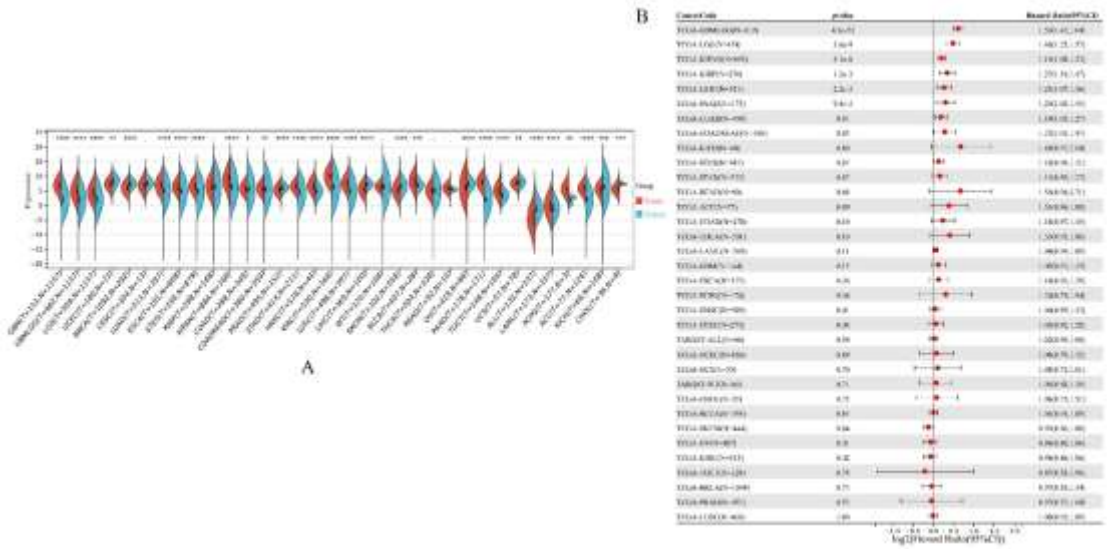

Figure 6: Pan-cancer analysis of IGFBP3 expression and its prognostic significance. (A-B): Evaluation of IGFBP3 expression levels and their association with prognosis across the 36 cancer types listed in the GTEx and TCGA databases.

Table 3, The prognosis of IGFBP3 in Pan-Cancer

Cohort	Hazard Ratio	p
TCGA-GBMLGG	1.53(1.42,1.64)	4.8e-31
TCGA-LGG	1.40(1.25,1.57)	3.6e-9
TCGA-LUAD	1.14(1.03,1.27)	0.01
TCGA-KIRP	1.27(1.10,1.47)	1.3e-3
TCGA-KIPAN	1.15(1.08,1.23)	5.1e-6
TCGA-COADREAD	1.22(1.01,1.47)	0.03

TCGA-THYM	2.36(1.24,4.49)	5.9e-3
TCGA-LIHC	1.21(1.07,1.36)	2.2e-3
TCGA-MESO	1.44(1.21,1.70)	2.3e-5
TCGA-PAAD	1.24(1.05,1.45)	9.8e-3
TCGA-SKCM	0.92(0.86,1.00)	0.04

4. Discussion

HCC accounts for 90% of primary liver malignancies and exemplifies the therapeutic challenges associated with the treatment of solid tumors. Targeted therapies focusing on the VEGF/PD-1 pathway result in only temporary responses, with a median PFS of <6 months, observed in only 19–30% of patients [15]. This therapeutic limitation is attributed to the molecular heterogeneity of HCC, as recent multi-omics analyses have categorized tumors into immune-exhausted, CTNNB1-mutant, and TP53-dysregulated subtypes, each possessing distinct therapeutic vulnerabilities [16]. Within this complex framework, we identified IGFBP3, a hepatotropic glycoprotein that regulates IGF-1/2 bioavailability, as a pan-subtype suppressor with strategic translational potential. Systemic downregulation of IGFBP3 in HCC is correlated with sex, tumor grade, age, and advanced TNM staging. Notably, IGFBP3 influences both OS and PFS in patients with HCC.

As a member of the insulin-like growth factor-binding protein family, IGFBP3 is the most prevalent IGF-binding protein in the bloodstream postnatally [17]. It plays a pivotal role in regulating cell proliferation, apoptosis, and differentiation, while reducing cancer development and affecting prognosis [17-18]. The expression of IGFBP3 varies among different cancer types. IGFBP3 demonstrates tumor-suppressive properties in breast cancer (low tissue expression correlating with increased premenopausal risk) [19-20], prostate cancer (reduced plasma levels and tumor growth inhibition upon overexpression) [21-23], and activated B-cell diffuse large B-cell lymphoma (ABC-DLBCL) [24]. Conversely, it exhibits oncogenic functions in advanced prostate cancer (mediating Olaparib resistance) [25] and cutaneous melanoma (SKCM, where low expression associates with poor prognosis).

Reflecting the context-dependent duality observed in breast cancer, prostate carcinoma, renal cell carcinoma, and lymphomas, IGFBP3 exhibits a biphasic tumor-modulatory role in HCC. Integrative analyses of our findings and published evidence indicates that IGFBP3 downregulation facilitates early hepatocarcinogenesis, whereas its overexpression associates with advanced tumor stage (III-IV), high-grade pathology (G3-G4), younger patient age (≤40 years), and significantly poorer prognosis in HCC. The stage-specific duality of IGFBP3—downregulation in early hepatocarcinogenesis versus overexpression in advanced HCC driving poor prognosis—is mediated by multiplexed molecular mechanisms. Based on the integrated analysis of TIMER and QUANTISEQ algorithms, IGFBP3 expression, and TCGA-LIHC pathway enrichment, we propose the following potential underlying mechanisms.

These mechanisms including: 1. IGF-Dependent Pathways: IGFBP3 sequesters IGF-1/2 ligands, thereby inhibiting the oncogenic PI3K/AKT and MAPK signaling pathways [26]. Its loss in HCC results in the derepression of these pathways, thereby accelerating tumorigenesis, a phenomenon also observed in breast (TCGA-BRCA) and prostate (TCGA-PRAD) cancers [27-28]. 2. Pro-Metastatic Signaling: In this study, GSEA revealed enrichment of TGF-β (ES = 0.5439) and MAPK (ES = 0.4385) pathways in IGFBP3-high tumors. TGF-β drives epithelial-mesenchymal transition (EMT) and stromal remodeling, whereas MAPK activation enhances metastatic potential [29]. IGFBP3 may amplify these pathways via direct interactions with TGF-β receptors or extracellular matrix components [30-31]. 3. Angiogenic Potential: Enrichment of IGFBP3-associated vascular smooth muscle contraction pathways (GSEA, ES = 0.4887) suggests neutrophil-derived VEGF-mediated angiogenesis [32]. 4. Immunomodulatory Role: Immune infiltration analysis revealed that IGFBP3 expression was significantly positively correlated with the abundance of multiple immune cell types, including M1 macrophages ($r = 0.37$, $p < 0.0001$), M2 macrophages ($r = 0.26$, $p < 0.0001$), and regulatory T cells (Tregs) ($r = 0.26$, $p < 0.0001$). This indicates that IGFBP3 possesses

broad immunocyte recruitment capabilities [33]. However, combined with the survival analysis results demonstrating that high IGFBP3 expression significantly predicts poor prognosis, we infer that despite the highest level of M1 macrophage infiltration, the concurrent presence of M2 macrophages and Tregs likely dominates the formation of an immunosuppressive microenvironment. This inhibitory milieu may compromise the potential anti-tumor functionality of M1 cells and collectively promote tumor immune escape, ultimately contributing to the unfavorable prognosis observed in patients with high IGFBP3 expression.

Although we found that IGFBP3 is lowly expressed in liver cancer, its overexpression is associated with a worse prognosis. However, we only collected a limited number of samples (8 pairs of HCC tissues and corresponding adjacent non-tumorous tissues) to validate IGFBP3 expression. Furthermore, the potential mechanism we proposed requires validation in in vivo and in vitro models, such as IGFBP3 knockdown in HCC cells or mouse systems. Our future research will focus on elucidating the stage-specific switching mechanism of IGFBP3.

5. Conclusion

In HCC, IGFBP3 expression is generally low. However, it is overexpressed in patients with advanced tumor stages (Stage III-IV), high pathological grades (G3-G4), and age <40 years, and this overexpression correlates with a poorer prognosis. This dual role – where low IGFBP3 expression promotes HCC development, while its overexpression drives tumor progression and poor prognosis – may involve mechanisms related to IGF-dependent pathways, pro-metastatic signaling, angiogenic potential, and immune modulation.

Acknowledgments: Not applicable

Author Contributions: Xu Y and Tao Y conceptualized and designed the study. Chen X, Li S, and Li W acquired, analyzed, and interpreted the data. Xu Y and Tao Y drafted the manuscript. All the authors critically revised the manuscript for its intellectual content.

Funding: This study was supported by the Scientific Research Project of Hunan Provincial Health Commission (NO. D202304017818) and the Hunan Provincial Natural Science Foundation (No. 2025JJ81027).

Data Availability: All data used in this study can be obtained by contacting the corresponding author via e-mail at 340468999@qq.com.

Ethics Approval and Consent to Participate: This study was approved by the Ethics Committee of Zhuzhou Central Hospital (NO. LLYPJ2025044-01).

Consent for Publication: Not applicable.

References

1. Bray F, Laversanne M, Sung H, Ferlay J, Siegel RL, Soerjomataram I, Jemal A. Global cancer statistics 2022: GLOBOCAN estimates of incidence and mortality worldwide for 36 cancers in 185 countries. CA Cancer J Clin. 2024 May-Jun;74(3):229-263.
2. Park JH, Koo BK, Kim W, Kim WH; Innovative Target Exploration of NAFLD (ITEN) Consortium. Histological severity of nonalcoholic fatty liver disease is associated with 10-year risk for atherosclerotic cardiovascular disease. Hepatol Int. 2021 Oct;15(5):1148-1159.
3. Huang DQ, El-Serag HB, Loomba R. Global epidemiology of NAFLD-related HCC: trends, predictions, risk factors and prevention. Nat Rev Gastroenterol Hepatol. 2021 Apr;18(4):223-238.
4. Schulze K, Imbeaud S, Letouzé E, Alexandrov LB, Calderaro J, Rebouissou S, et al. Exome sequencing of hepatocellular carcinomas identifies new mutational signatures and potential therapeutic targets. Nat Genet. 2015 May;47(5):505-511.
5. Llovet JM, Kelley RK, Villanueva A, Singal AG, Pikarsky E, Roayaie S. et al. Hepatocellular carcinoma. Nat Rev Dis Primers. 2021 Jan 21;7(1):6.
6. Finn RS, Qin S, Ikeda M, Galle PR, Ducreux M, Kim TY, et al. Atezolizumab plus Bevacizumab in Unresectable Hepatocellular Carcinoma. N Engl J Med. 2020 May 14;382 (20):1894-1905.
7. Villanueva A. Hepatocellular Carcinoma. N Engl J Med. 2019 Apr 11;380(15):1450-14 62.
8. Kacar Z, Slud E, Levy D, Candia J, Budhu A, Forgues M, et al. Characterization of tumor evolution by functional clonality and

phylogenetics in hepatocellular carcinoma. Commun Biol. 2024 Mar 29;7(1):383.
9. Xu C, Xu Z, Zhang Y, Evert M, Calvisi DF, Chen X. β-Catenin signaling in hepatocellular carcinoma. J Clin Invest. 2022 Feb 15;132(4):e154515.
10. Varma Shrivastav S, Bhardwaj A, Pathak KA, Shrivastav A. Insulin-Like Growth Factor Binding Protein-3 (IGFBP-3): Unraveling the Role in Mediating IGF-Independent Effects Within the Cell. Front Cell Dev Biol. 2020 May 5;8:286.
11. Johnson MA, Firth SM. IGFBP-3: a cell fate pivot in cancer and disease. Growth Horm IGF Res. 2014 Oct;24(5):164-73.
12. Liu S, Li C, Wang H, Wang S, Yang S, Liu X, Yan J, Li B, Beatty M, Zastrow-Hayes G, Song S, Qin F. Mapping regulatory variants controlling gene expression in drought response and tolerance in maize. Genome Biol. 2020 Jul 6;21(1):163. doi: 10.1186/s13059-020-02069-1. PMID: 32631406; PMCID: PMC7336464.
13. Liu S, Li C, Wang H, Wang S, Yang S, Liu X, et al. Mapping regulatory variants controlling gene expression in drought response and tolerance in maize. Genome Biol. 2020 Jul 6;21(1):163.
14. Finotello F, Mayer C, Plattner C, Laschober G, Rieder D, Hackl H, et al. Molecular and pharmacological modulators of the tumor immune contexture revealed by deconvolution of RNA-seq data. Genome Med. 2019 May 24;11(1):34.
15. Wang J, Yu H, Dong W, et al. N6-Methyladenosine-Mediated Up-Regulation of FZD10 Regulates Liver Cancer Stem Cells' Properties and Lenvatinib Resistance Through WNT/β-Catenin and Hippo Signaling Pathways. *Gastroenterology*. 2023; 164(6):990-1005.
16. Llovet JM, Willoughby CE, Singal AG, et al. Nonalcoholic steatohepatitis-related hepatocellular carcinoma: pathogenesis and treatment. *Nat Rev Gastroenterol Hepatol*. 2023;20(8):487-503.
17. C Bhardwaj A, Pathak KA, Shrivastav A, Varma Shrivastav S. Insulin-Like Growth Factor Binding Protein-3 Binds to Histone 3. *Int J Mol Sci*. 2021;22(1):407.
18. Shen C. ID1 and IGFBP3: roles in cellular senescence, cardiac development, angiogenesis and cancer diagnosis. *J Transl Med*. 2023;21(1):797.
19. Scully T, Firth SM, Scott CD, et al. Insulin-like growth factor binding protein-3 links obesity and breast cancer progression . *Oncotarget*. 2016;7(34):55491-55505.
20. McIntosh J, Dennison G, Holly JM, et al. IGFBP-3 can either inhibit or enhance EGF-mediated growth of breast epithelial cells dependent upon the presence of fibronectin. *J Biol Chem*. 2010;285(50):38788-38800.
21. Mehta HH, Gao Q, Galet C, Paharkova V, Wan J, Said J, Sohn JJ, Lawson G, Cohen P, Cobb LJ, Lee KW. IGFBP-3 is a metastasis suppression gene in prostate cancer. Cancer Res. 2011 Aug 1;71(15):5154-63.
22. Devi GR, Sprenger CC, Plymate SR, Rosenfeld RG. Insulin-like growth factor binding protein-3 induces early apoptosis in malignant prostate cancer cells and inhibits tumor formation in vivo. *Prostate*. 2002;51 (2):141-152.
23. Fang P, Hwa V, Little BM, Rosenfeld RG. IGFBP-3 sensitizes prostate cancer cells to interferon-gamma-induced apoptosis. *Growth Horm IGF Res*. 2008;18 (1):38-46.
24. Li HB, Wang D, Zhang Y, Shen D, Che YQ. IGFBP3 Enhances Treatment Outcome and Predicts Favorable Prognosis in ABC-DLBCL. *J Oncol*. 2023;2023:1388041.
25. Leslie AR, Ning S, Armstrong CM, et al. IGFBP3 promotes resistance to Olaparib via modulating EGFR signaling in advanced prostate cancer. *iScience*. 2024;27(2):108 98 4.
26. Liu Y, Lv H, Li X, et al. Cyclovirobuxine inhibits the progression of clear cell renal cell carcinoma by suppressing the IGFBP3-AKT/STAT3/MAPK-Snail signalling pathway [published correction appears in Int J Biol Sci. 2024 Dec 1;20(15):6279-6280.
27. Scully T, Firth SM, Scott CD, et al. Insulin-like growth factor binding protein-3 links obesity and breast cancer progression . *Oncotarget*. 2016;7(34):55491-55505.
28. Ragavi R, Muthukumaran P, Nandagopal S, et al. Epigenetics regulation of prostate cancer: Biomarker and therapeutic potential. *Urol Oncol*. 2023;41(8):340-353.
29. Hao Y, Baker D, Ten Dijke P. TGF-β-Mediated Epithelial-Mesenchymal Transition

and Cancer Metastasis. *Int J Mol Sci*. 2019; 20(11):2767.
30. Zhang X, Wang G, Gong Y, et al. IGFBP3 induced by the TGF-β/EGFRvIII transactivation contributes to the malignant phenotype of glioblastoma. *iScience*. 2023;26 (5):106639.
31. Varma Shrivastav S, Bhardwaj A, Pathak KA, Shrivastav A. Insulin-Like Growth Factor Binding Protein-3 (IGFBP-3): Unraveling the Role in Mediating IGF-Independent Effects Within the Cell. *Front Cell Dev Biol*. 2020;8:286.
32. Granata R, Trovato L, Lupia E, et al. Insulin-like growth factor binding protein-3 induces angiogenesis through IGF-I- and SphK1-dependent mechanisms. *J Thromb Haemost*. 2007;5(4):835-845.
33. Chen S, Liu J, Zhang S, et al. Deciphering m6A signatures in hepatocellular carcinoma: Single-cell insights, immune landscape, and the protective role of IGFBP3. *Environ Toxicol*. 2025;40(3):367-383.